Polymerization of Olefins through Heterogeneous Catalysis. VIII. Monomer Sorption Effects

R. A. HUTCHINSON and W. H. RAY,* *Department of Chemical Engineering, University of Wisconsin-Madison 1415 Johnson Drive, Madison, WI 53706*

Synopsis

In solid catalyzed olefin polymerization, equilibrium sorption plays a key role in determining the local monomer concentration(s) in the semicrystalline polymer shell which surrounds the active sites of the catalyst surface. Modelling based on polymer solution thermodynamics indicates that crystallinity and reactor environment have a major effect on this local monomer concentration. The model is used to explain well known experimental trends seen in the literature, such as observed differences in gas phase and diluent slurry polymerization rates, and enhanced α-olefin incorporation in gas phase copolymerization.

INTRODUCTION

The polymerization of olefins over solid catalysts is a complex reaction, involving both physical and kinetic effects. On a kinetic level, the reaction can involve multiple active sites on the catalyst surface, with each site having its own rates of activation, polymerization, and deactivation. Often electron donors are added to further modify the kinetic behaviour of the sites. On a physical level, the reaction involves the breakup of the original catalyst particle and the dispersion of catalyst fragments in the growing polymer particle, the sorption and diffusion of reactants through the polymer to the catalyst surface, and the removal of heat of polymerization generated at the catalyst surface. Because of these complexities, experimental results can often be explained by both physical and kinetic arguments.

In an attempt to resolve these questions and better understand the polymerization process, recent efforts have been made to quantify the physical model of polymer growth over which a reasonable kinetic model can be superimposed.[1-3] Figure 1 shows a schematic of the multigrain model of particle growth. Because of the dispersion of catalyst fragments throughout the polymer particle, two levels of diffusion exist. Reactants first diffuse on a macro level, between the catalyst fragments which are each surrounded by a shell of semicrystalline polymer. At the surface of the microparticles, reactants must sorb into the polymer phase, then diffuse through the polymer to the catalyst surface. There is ample physical evidence supporting this model of polymer growth.[4-6]

* To whom correspondence should be addressed.

Journal of Applied Polymer Science, Vol. 41, 51–81 (1990)
 CCC 0021-8995/90/1-20051-31$04.00

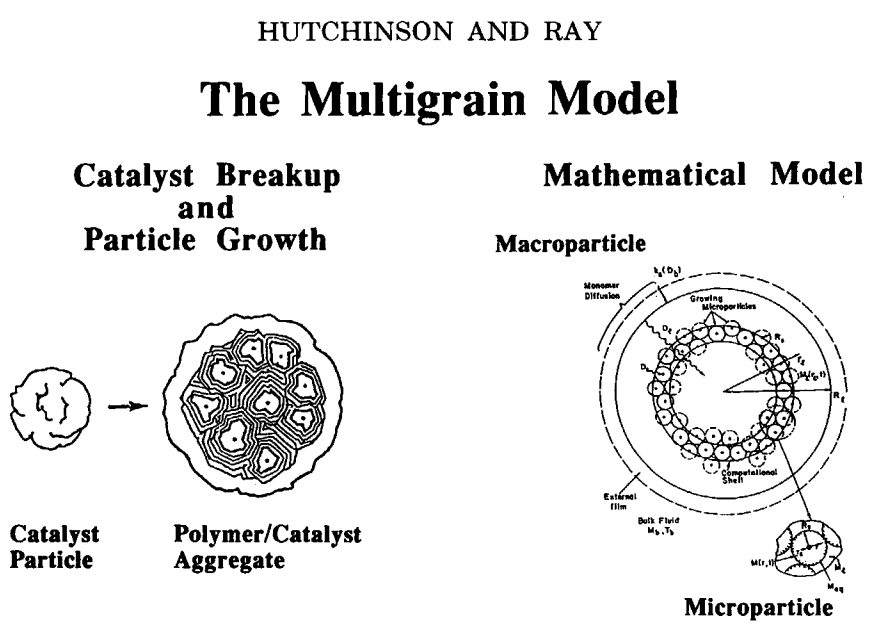

Fig. 1. The multigrain model: A mathematical representation of polymer particle growth.

Much of the previous work of Floyd et al. has concentrated on the diffusion aspects of the multigrain model. It is believed that the sorption process—the solubilization of the reactants in the polymer phase—is an important one. The thermodynamics of monomer sorption in crystalline polyolefins control the monomer accessibility to the catalyst surface, and thus the rate of polymerization. This paper will examine the sorption process for both gas and liquid phase environments, and apply the theory to explain experimental trends seen in the olefin polymerization literature.

OVERVIEW OF SORPTION THEORY

Solubility of penetrants, either gas, vapour or liquid, into crystalline polymer is dependent on the properties of both the penetrant and the polymer. For sparingly soluble penetrants, sorption can be modelled by Henry's law; the amount sorbed is sufficiently small so that the polymer matrix does not undergo any swelling strain or other rearrangment during the sorption process. However, as penetrants reach higher concentrations the situation becomes more complex due to increased penetrant-polymer interactions. The sorbed penetrant swells and plasticizes the polymer, leading to increased mobility for both the polymer segments and penetrant molecules. This can even alter the morphology of the polymer.[7]

For crystalline polymers, sorption occurs only within the amorphous regions of the polymer, both for highly soluble vapours and liquids[8] as well as for sparingly soluble gases.[9] Thus, solubility data presented in this paper will be in terms of moles of penetrant per unit volume amorphous polymer ($[M]^*$); actual concentrations depend on the crystallinity of the polymer according to

$$[M] = \alpha_v [M]^* \tag{1}$$

The amorphous volume fraction, α_v, can be determined from polymer density, ρ, according to the relation

$$\alpha_v = \frac{\rho_c - \rho}{\rho_c - \rho_a} \tag{2}$$

where ρ_c and ρ_a are densities of crystalline and amorphous polymer, respectively. Although sorption occurs only in the amorphous phase, polymer crystallinity does play an important role in the process. The crystallites tie the amorphous regions of polymer together and limit the amount of swelling. This effect is especially important for highly soluble vapours and liquids. Most studies deal with sorption in polyethylene, but the results can be applied to other polyolefins including copolymers. The primary effect of comonomer is to reduce crystallinity and this can be important. However, experimental data indicates that for amorphous copolymers such as ethylene-propylene rubbers, the comonomer content has very little effect on sorption properties.[10,11]

Much of the sorption modelling discussed below is based on the Flory-Huggins theory of polymer solutions, which provides an estimate of solvent activity above an amorphous polymer. For long-chain polymer molecules the relation is

$$\ln(a_1) = \ln(v_1) + v_p + \chi_{1p}(v_p)^2 \tag{3}$$

where v_1 and v_p are volume fractions of solvent and polymer, respectively, and χ_{1p} is the interaction parameter between the two. The solvent activity in the vapour, a_1, is usually characterized as P_1/P_1^0, where P_1^0 is the vapour pressure of pure liquid solvent and P_1 is the partial pressure of the vapour above the polymer.

VAPOUR SORPTION IN CRYSTALLINE POLYMERS

Single Component

Vapour sorption is usually expressed in terms of the pressure of the vapour above the polymer, according to

$$[M_1]^* = k^* P_1 \tag{4}$$

For permanent gases, such as O_2 or CO_2, penetrant sorption is minimal and k^* is a Henry's law constant, independent of both pressure and volume fraction. Henry's law can be simplified from Flory-Huggins theory, assuming $v_p \approx 1$. Equation (3) becomes

$$\ln\left(\frac{P_1}{P_1^0}\right) = \ln(v_1) + 1.0 + \chi_{1p} \tag{5}$$

or

$$v_1 = \frac{P_1}{P_1^0[\exp(1 + \chi_{1p})]} \tag{6}$$

a form of Henry's law. It has been shown experimentally that this simple relation is applicable to low molecular weight hydrocarbon vapours sorbed in polyolefins, such as ethylene and propylene. Li and Long[12] examined the solubility of ethylene in polyethylene up to 90 atm at 25°C. Although they found deviations from Henry's law at high pressures, they concluded Henry's law was applicable up to the critical pressure of ethylene, as shown by Curve 1 in Figure 2. Michaels and Bixler[9] found that ethane, propane and propylene sorbed in polyethylene obeyed Henry's law throughout the range of their experimental investigation (5–55°C, < 1 atm), as did Kulkarni and Stern[13] for ethylene and propane sorption in polyethylene (5–35°C, < 40 atm).

Henry's law is generally not applicable for heavier hydrocarbon vapours which tend to swell and plasticize the polymer to a much greater extent. In this case the solubility of the penetrant is no longer independent of pressure, but becomes a function of penetrant concentration, as shown in Figure 3.[14] The relationship is often modelled according to

$$k^* = k_H^* \exp(\sigma[M]^*) \tag{7}$$

where k_H^* is the penetrant solubility in the amorphous polymer at zero concen-

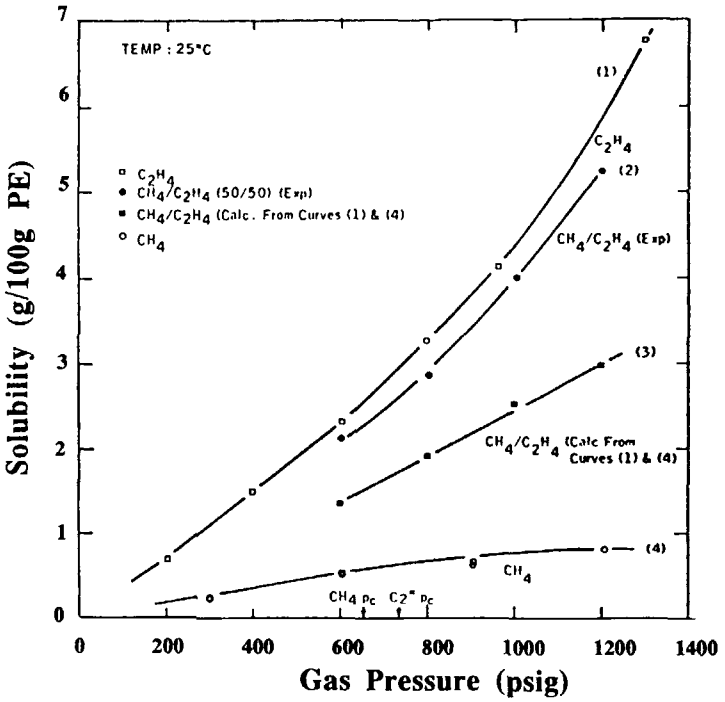

Fig. 2. Solubility of methane and ethylene vapour in LDPE at 25°C.[12]

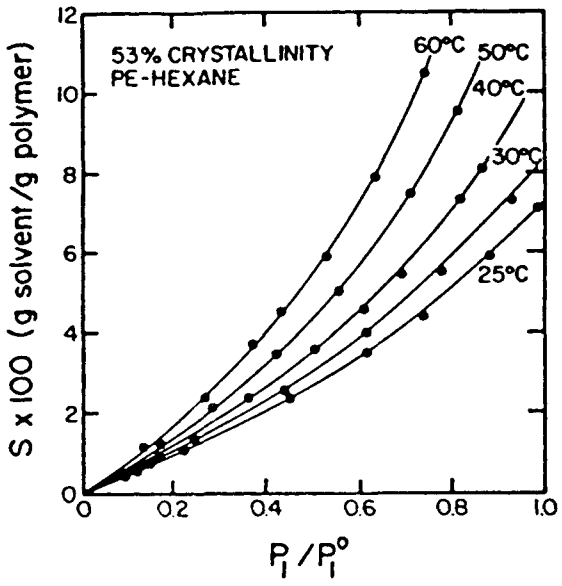

Fig. 3. Solubility of hexane vapour in 53% crystalline LDPE as a function of vapour activity.[14]

tration and σ is a proportionality constant. This semi-empirical relationship can also be derived from the Flory-Huggins equation.[10] At low penetrant concentrations, as $[M]^*$ approaches zero, a Henry's law constant can be estimated for these heavier vapours.

Literature values of Henry's law constants for hydrocarbons in polyethylene from nine different sources have been compiled and tabulated in Table I. The data are for straight chain paraffins methane to octane, as well as for ethylene and propylene. For the heavier hydrocarbons, the data reflect the penetrant solubility coefficient as $[M]^*$ approaches zero. In the literature, attempts have been made to correlate these constants with temperature and penetrant properties. Most of the work makes use of the fact that amorphous polyethylene acts as a liquid-like matrix in which the vapour condenses.

Michaels and Bixler,[9] and later Teplyakov and Durgar'yan,[15] correlated penetrant solubility at a reference temperature (25°C) to the Lennard-Jones molecular force constant (ϵ/k) in the form

$$\log(k_0^*) = a + b\left(\frac{\epsilon}{k}\right) \tag{8}$$

The temperature effect was modelled according to the van't Hoff relation

$$k^* = k_0^* \exp\left(\frac{-\Delta H_s}{RT}\right) \tag{9}$$

TABLE I
Henry's Law Amorphous Polymer Solubility Coefficients for Vapour Sorption in Semi Crystalline Polyethylene

Reference	PE density (g/cm^3)	Vol frac amorphous	Penetrant	Temp (deg C)	Henry's law const (mol/ L-amorp/atm)
Li and Long[12]	0.9327	0.49	methane	25.0	0.0136
			ethylene	25.0	0.0373
Michaels and Bixler[9]	0.909	0.58	methane	25.0	0.0091
	0.948	0.31	ethane	25.0	0.0570
	0.962	0.22	propane	25.0	0.1770
			propylene	25.0	0.1580
Kulkarni and Stern[13]	0.918	0.55	methane	5.0	0.0082
				20.0	0.0080
				35.0	0.0082
			ethylene	5.0	0.0461
				20.0	0.0392
				35.0	0.0324
			propane	5.0	0.2400
				20.0	0.1970
				35.0	0.1660
Eby[53]			ethane	23.0	0.0550
MacDonald and Huang[51]	0.9203	0.54	methane	40.0	0.0133
			ethane	40.0	0.0367
			propane	40.0	0.2210
Rogers et al.[8]	0.922	0.52	pentane	25.0	2.0430
	0.938	0.39	hexane	0.0	18.2300
	0.954	0.3		25.0	6.0600
				30.0	5.3900
			heptane	25.0	18.7200
			octane	25.0	53.9600
Castro et al.[52]	0.915	0.57	butane	0.0	1.1440
				20.0	0.5730
				40.0	0.3260
			pentane	0.0	4.4000
				20.0	1.8600
				35.0	1.0900
			hexane	10.0	9.5700
				20.0	5.8900
				35.0	3.1000
			heptane	15.0	23.1500
				25.0	14.0200
				40.0	6.9200
Takeuchi and Okamura[48]	0.9208	0.53	hexane	15.0	8.0000
				25.0	7.2300
				35.0	6.2600
Robeson and Smith[19]	0.9238	0.51	ethane	30.0	0.0649
				40.0	0.0609
				50.0	0.0550
				60.0	0.0523
			butane	30.0	0.6750
				40.0	0.5520
				50.0	0.4370
				60.0	0.3850

where

$$\Delta H_s = c + d\left(\frac{\epsilon}{k}\right) \tag{10}$$

ΔH_s includes both the heat of condensation and the heat of mixing. The values of constants a–d are dependent only on the nature of the polymer, not on penetrant properties.

A similar correlation, discussed in a paper by Abraham et al.,[16] relates sorption of a penetrant in polymer to its solubility in hexadecane according to

$$\log(k_0^*) = a + b\log(L_{16}) \tag{11}$$

$$\Delta H_s = c + d\log(L_{16}) \tag{12}$$

where L_{16} is the Ostwald solubility coefficient of the penetrant in hexadecane. This correlation fits the data equally as well as eqs. (8) and (10).

Stern et al.[17] observed that Henry's Law coefficients increase with the critical temperature (T_c) of the penetrants, and decrease as the actual temperature increases. The experimental data show that when $\log(k^*)$ is plotted against (T_c/T), the relationship is nonlinear. Based on this observation, the correlation

$$\log(k^*) = a + b(T_c/T)^2 \tag{13}$$

was proposed and found to fit literature data well. Equation (13) fit the data of Table 1 better than the other correlations, with the form

$$\log(k^*) = -2.38 + 1.08(T_c/T)^2 \tag{14}$$

Figure 4 shows that the fit is good for values of k^* spanning several orders of magnitude. This method of corresponding states has two other advantages, as mentioned by Stern: values of T_c are more readily available and are a more fundamental molecular property than (ϵ/k) values, and the temperature dependence of k^* is built into the correlation.

Stern et al.[17] also proposed a correlation to estimate the point at which departures from Henry's law become noticeable because of the plasticizing effect of the penetrant. Defining P_{dev} as the pressure at which a 5% deviation from Henry's law solubility would occur, and using available experimental evidence, the following relationship was proposed

$$\log\left(\frac{P_{\text{dev}}}{P_c}\right) = 3.025 - 3.50\left(\frac{T_c}{T}\right) \tag{15}$$

This expression is useful in defining where more complex thermodynamic relationships must be used to predict sorption.

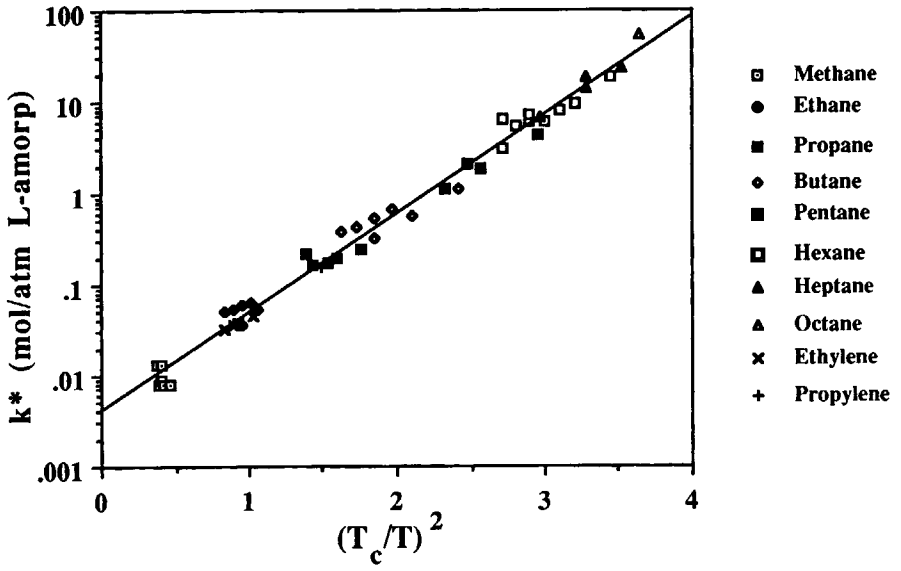

Fig. 4. Henry's law solubility coefficients: Correlation of Stern[17] (data taken from Table I).

Vapour Mixtures

For vapour mixtures, it is necessary to determine whether the presence of one component leads to increased sorption of other components. If all gases or vapours have weak interactions with polymer, they will sorb independently, depending on the partial pressure of each gas. Meyer[18] shows experimentally that the presence of CO_2 does not affect the sorption of O_2 or N_2. However, even for low molecular weight organic vapours, some interaction occurs. Figure 2 shows data of Li and Long[12] for pure component ethylene and methane sorption at 25°C, and for a 50–50 mixture of the two components. Sorption of the more soluble ethylene enhances the solubility of the mixture well above that predicted from independent sorption. The relative composition of the sorbed vapour mixture in the polymer was not determined in their work.

Only one study could be found which examined the relative solubilities of a vapour mixture in polyethylene. Robeson and Smith[19] examined sorption of an ethane-butane mixture in LDPE at atmospheric pressure. This pressure is below the Henry's law deviation pressure predicted by eq. (15) for ethane, but slightly above the predicted P_{dev} for the butane component at the lower temperatures in the range examined. Figure 5a shows that at 40, 50, and 60°C, the ethane sorption is not affected by the presence of butane in the mixture (i.e. k^* for ethane is independent of butane partial pressure). However, at 30°C, where the concentration of sorbed butane in the polymer is higher, some effect is seen; the ethane solubility coefficient increases 10% as the butane mole fraction in the vapour mixture increases from zero to one. The polymer swelling caused by the butane leads to enhanced sorption of the ethane. The effect is slight and only seen at 30°C; however, at increased pressures it should become more pronounced due to increased butane concentrations.

Figure 5b shows the sorbed butane to ethane concentration ratio in the polymer relative to the bulk mixture ratio, according to

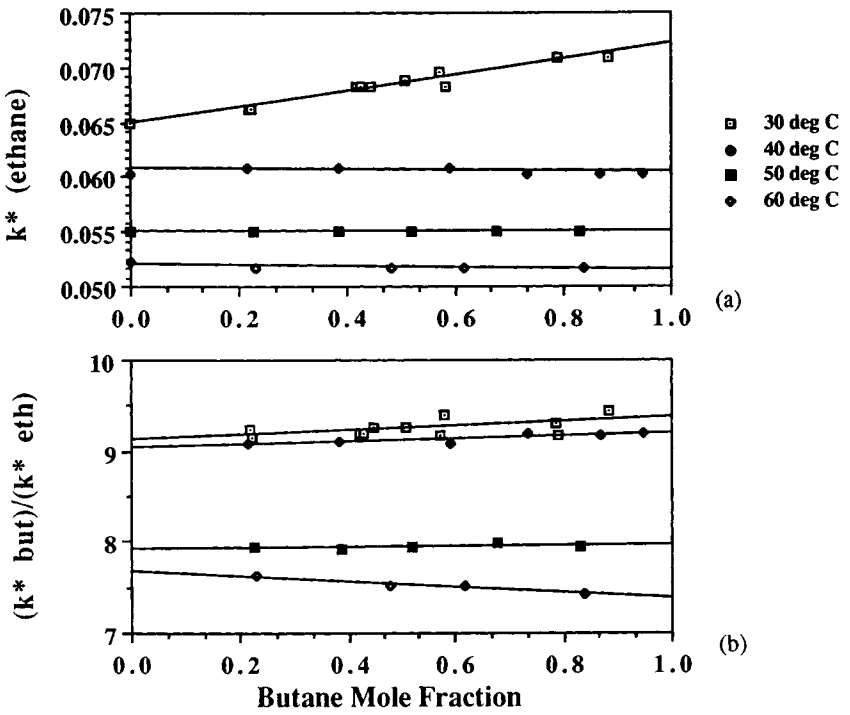

Fig. 5. Solubility of ethane-butane vapour mixture in LDPE (data taken from Robeson and Smith.[19] $P = 1$ atm: (a) Ethane solubility coefficient $\left(\frac{\text{mol}}{(\text{atm})(\text{L-amorp})}\right)$ versus butane mole fraction. (b) Solubility coefficient ratio versus butane mole fraction.

$$R = \frac{([M_{but}]^*/[M_{eth}]^*)}{([M_{but}]_b/[M_{eth}]_b)} = \frac{k^*_{but}}{k^*_{eth}} \tag{16}$$

It can be seen that the heavier butane component is preferentially sorbed by a factor of 7.5 to 9.5, with R decreasing as temperature increases. This trend is predicted adequately by eq. (14). The ratio is independent of mixture composition, indicating that the enhanced sorption seen for ethane at 30°C also occurs for the butane fraction. This is not surprising; the plasticizing effect of the sorbed butane leads to increased sorption for both components.

These data show the assumption that mixture components sorb independently of each other is not a good one. At best it can only give a rough idea of the relative concentration of the sorbed components. In general, the sorption of a heavier penetrant will lead to polymer swelling and enhanced sorption of the lighter penetrant. The relative swelling between the two components, however, appears to be independent of composition.

Application to Olefin Polymerization

Equation (14) will be used in this work to estimate the solubility of olefin monomers in growing polyolefin particles. In Figure 6a, the Henry's law solu-

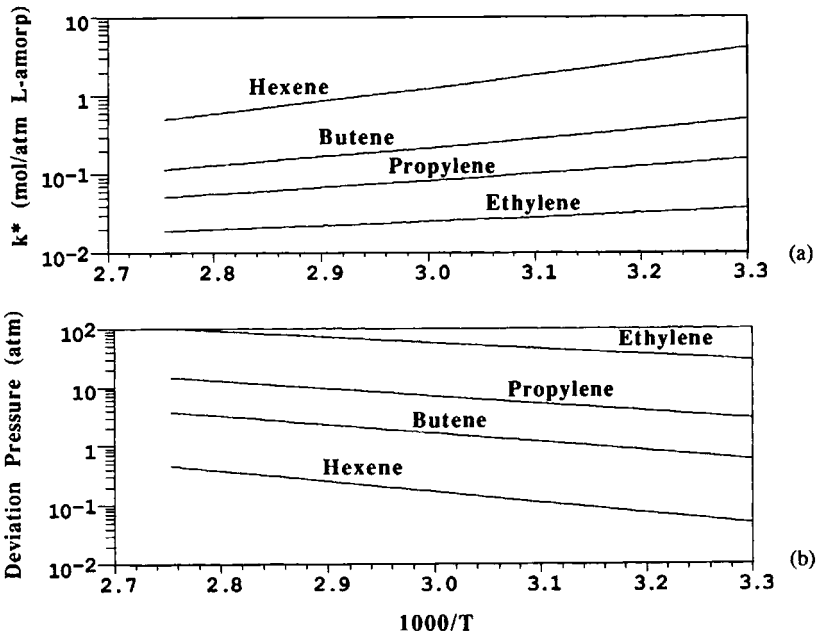

Fig. 6. Olefin vapour solubility in amorphous polyolefin as a function of inverse temperature: (a) Henry's law solubility coefficient $\left(\frac{\text{mol}}{(\text{atm})(\text{L-amorp})}\right)$ (b) Predicted pressure (atm) for 5% deviation from Henry's law behaviour.

bility coefficient is shown as a function of temperature for ethylene, propylene, butene and hexene. The heavier penetrants, such as butene and hexene, sorb an order of magnitude more than ethylene.

Equation (15) was used in the construction of Figure 6b, a plot of deviation pressure versus 1/T for the monomers. It can be seen that Henry's law will always be valid for typical ethylene polymerization conditions (30–90°C, < 40 atm), but will not be valid for butene and hexene comonomers. Propylene is a borderline case; the assumption of Henry's law may slightly underestimate sorbed concentration, but not to a significant degree.

It is expected that the presence of a heavier comonomer which deviates from Henry's law behaviour (i.e. $P > P_{dev}$) will lead to enhanced sorption of the lighter monomer, relative to the homopolymerization case. This effect may help explain enhanced copolymerization rates sometimes seen during gas phase polymerization, as will be discussed in more detail later. Note that the ratio of comonomer to monomer in the polymer phase is much higher than that in the vapour mixture; this is a significant factor when considering comonomer incorporation.

LIQUID SORPTION IN CRYSTALLINE POLYMERS

Single Component

According to theory[20] liquid sorption should be identical to saturated vapour sorption for a single component ($a_1 = 1$). However, experimentally, this is not

always observed. Figure 7 shows experimental data from four sources for the sorption of hexane in LDPE at various temperatures; two from saturated vapour data (see Fig. 3) and two from liquid sorption data. The data are plotted in terms of the volume fraction of hexane in the swollen amorphous phase of the polymer. It is apparent that the amount of liquid hexane sorbed in the polymer is substantially higher than the amount of saturated vapour sorbed at the same temperature. In the following discussion, only the liquid sorption data will be used.

Although extent of sorption will be expressed on a crystallite-free basis in this paper, polymer crystallinity plays an important role in determining the value. Crystallites act as giant crosslinks, limiting the amount of swelling. Completely amorphous polyolefins, such as ethylene-propylene rubber (EPR), will dissolve in a good solvent such as hexane; in crystalline polyolefins the presence of the crystallites prevents this from occurring. Flory-Huggins theory (eq. 3) does not take into account the "elastic" restraining effects of the crystallites.

Experimental studies examining liquid sorption in polyolefins are limited. Table II summarizes the data that were found. The measurement of data has a degree of uncertainty due to the difficulty in determining the point at which the polymer loses its surface film of liquid.[21] This uncertainty is reflected in the data presented in Table II and Fig. 7.

For these systems, sorption is often examined in terms of the difference in the solubility parameter of the liquid and the polymer. The solubility parameter is a measure of the cohesive energy density of a component; components with similar solubility parameters are apt to be mutually compatible. Michaels et al.[22] have shown a linear relationship between $|\Delta\delta|$ and extent of sorption of various solvents in polypropylene (PP) at 40°C. In order to examine this relationship further, it is necessary to estimate the solubility parameters for both polymer and liquid.

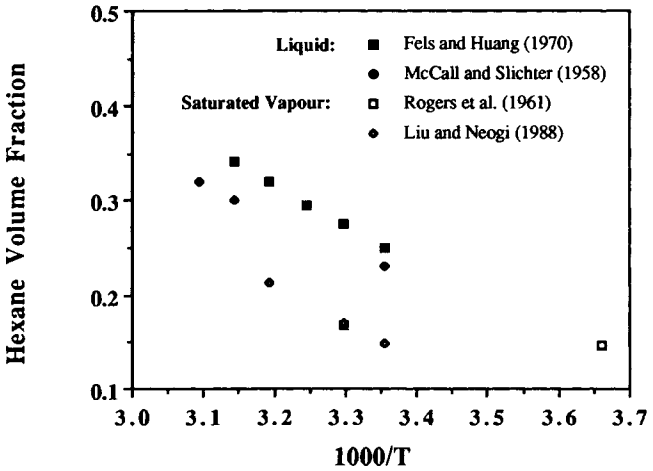

Fig. 7. Liquid and saturated vapour sorption of hexane in LDPE: Volume fraction hexane in swollen amorphous phase versus inverse temperature.

TABLE II
Liquid Sorption in Polyolefins

Reference/system	Penetrant	Temperature (°C)	v_1 (cm^3 penetrant per cm^3 swollen amorphous polymer)	$\delta_{penetrant}$ $(cal/cm^3)^{1/2}$	$\lvert\Delta\delta\rvert$ $(cal/cm^3)^{1/2}$
Long[41]	heptane	0.0	0.318	7.430	0.623
PP		40.0	0.398	7.051	0.528
Amorphous wt frac		50.0	0.424	6.951	0.507
= 0.26		60.0	0.443	6.484	0.489
	toluene	0.0	0.321	9.270	1.207
		40.0	0.389	8.880	1.301
		50.0	0.432	8.780	1.322
		60.0	0.465	8.680	1.343
Fels and Huang[21]	hexane	25.0	0.251	7.070	0.691
LDPE		30.0	0.275	7.016	0.684
Amorphous vol frac		35.0	0.296	6.963	0.678
= 0.57		40.0	0.321	6.907	0.672
		45.0	0.342	6.851	0.668
	benzene	25.0	0.234	8.880	1.119
		30.0	0.271	8.820	1.120
		35.0	0.304	8.770	1.130
		40.0	0.335	8.720	1.141
		45.0	0.349	8.660	1.141
McCall and Slichter[40]	hexane	25.0	0.231	7.070	0.691
LDPE		30.0	0.275	7.016	0.684
Amorphous vol frac		45.0	0.300	6.851	0.668
= 0.57		50.0	0.320	6.796	0.662

For semi-crystalline polyolefins at room temperature, the value of 8.1 $(cal/cc)^{1/2}$ is commonly used for the solubility parameter of PP and 7.9 for PE.[23,24] Ito and Guillet[11] measured similar values for amorphous polyolefins, but found that the solubility parameter is a function of temperature. This seems reasonable; as temperature increases so does the energy content of the polymer. For amorphous EPR, a value of 7.70 $(cal/cc)^{1/2}$ was observed at 30°C, while at 73°C the value was 7.18. In this work it will be assumed that the parameter is linear with temperature, according to the equation

$$\delta_p = 7.70 - 0.0121(T - 303.15) \tag{17}$$

Ito and Guillet found that the value of δ_p did not change with the polyolefin composition—the value for amorphous PP at 30°C was 7.67, very close to the EPR value at the same temperature. Thus, eq. (17) will be used for all olefin polymers and copolymers.

For liquids, the solubility parameter for temperatures well below the boiling point is often estimated as

$$\delta = \sqrt{\frac{\Delta H_{vap} - RT}{V}} \tag{18}$$

However, this equation is not applicable for temperatures close to or above the normal boiling point of the liquid.[24] This fact becomes important when deter-

mining solubility parameters for the low boiling point olefin monomers. A correlation suggested by Bradford and Thodos[50] is valid up to critical temperatures

$$\delta = \delta_c + a(1 - T_r)^b \tag{19}$$

The δ values for seventeen hydrocarbons are fit well by this correlation over a wide temperature range. The constants δ_c, a and b are tabulated by Bradford and Thodos for different components, including many paraffins, ethylene and propylene. For all paraffins other than methane, $a = 7.41$ and $b = 0.447$; for olefins, the values of a and b differ slightly.

As mentioned previously, Michaels et al.[22] found a linear relationship between $|\Delta\delta|$ and volume fraction solvent, v_1, at a temperature of 40°C. Using eqs. (17) and (19), values of $|\Delta\delta|$ have been estimated for the data of Table II and are included as part of the table. No general relationship can be seen between v_1 and $|\Delta\delta|$. Therefore, in this work the experimental data of Long[41] are used to estimate the sorption of heptane in PP; Figure 8a shows a cubic fit of v_p in terms of inverse temperature. Figure 8b is a similar plot for the hexane-LDPE system; because of the scatter in the data a linear relationship is assumed. Since the curves are empirical fits of experimental data, extrapolation is not recommended.

Liquid Mixtures

As with vapour mixtures, the consideration of liquid mixtures adds another level of complexity to the above discussion. Not only is the amount of swelling

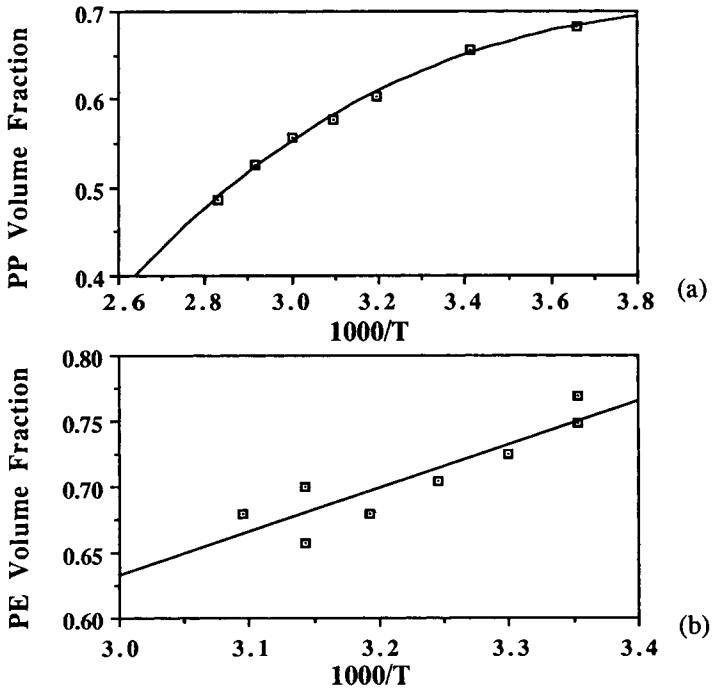

Fig. 8. (a) Polypropylene volume fraction in heptane swollen amorphous polymer (data of Long[41]) (b) Polyethylene volume fraction in hexane swollen amorphous polymer.[21,40]

caused by the mixture important, but the partition of the two liquids in the swollen polymer must also be determined. In olefin production, the polymerization is often carried out in a liquid mixture, with the olefin monomer dissolved in an inert diluent. It is important to be able to determine the relative solubilities of the monomer and diluent as they sorb into the polymer phase. Mixture effects can be important, as illustrated by Fels and Huang,[25] who examined the permeation of benzene-hexane mixtures through LDPE. It was found that a 50-50 mixture of benzene-hexane showed enhanced permeability through a LDPE film, compared to each of the two liquids alone. The relative concentration of the liquids in the polymer phase was not measured.

Theory has been developed in order to estimate the partition of two liquids in a crosslinked polymer by Krigbaum and Carpenter.[26] The development assumes that all of the polymer is in one phase—for olefin polymerization this is equivalent to neglecting the effects of any soluble polymer fraction dissolved in the liquid diluent. Using the lattice theory of Flory and a free energy balance, the derivation leads to the following equation for the partition coefficient K:

$$-\ln(K) = (1.0 - j)\ln\left(\frac{v_2}{\phi_2}\right) + 2.0\chi_{12}(v_2 - \phi_2) + J \tag{20}$$

where

$$K = \frac{(v_1/v_2)}{(\phi_1/\phi_2)}$$

$$J = (\chi_{12} + \chi_{1p} - j\chi_{2p})v_p$$

$$j = \frac{V_1}{V_2}$$

ϕ_1, ϕ_2 = binary volume fractions of components in liquid phase
v_1, v_2, v_p = ternary volume fractions in amorphous polymer
V_1, V_2 = partial molar volumes in the binary liquid mixture
χ_{ij} = Flory interaction parameter for $i - j$ mixture

A partition coefficient (K) of unity indicates that the two solutes maintain the same volume fraction ratio in the polymer phase as they have outside the polymer. As mentioned by Gardon,[27] the derivation of eq. (20) contains no assumption which limits it to bulk swelling of crosslinked polymers; the extent of swelling is expressed by the parameter v_p. Thus it can be applied to crystalline polymers for which the crystallites act as crosslinks and control the amount of swelling. With knowledge of v_p, the interaction parameters, and the partial molar volumes of the two liquids, it is possible to solve for the volume fraction of the two liquids in the polymer phase as a function of their volume fractions in the binary liquid phase. This theory has been applied to emulsion polymerization,[27,28] but not, as far as we know, to catalyzed olefin polymerization.

Application to Olefin Polymerization

In order to apply Krigbaum-Carpenter (K-C) theory to olefin polymerization, it is necessary to obtain estimates for a number of parameters. This section

will discuss how these parameters are estimated, apply K-C theory to propylene polymerization in heptane diluent, and bring forward some possible limitations in the application of the theory to olefin polymerization.

In eq. (20), three Flory interaction parameters are found. These parameters are a measure of the favorability of forming contacts between each pair of components. The equation

$$\chi_{ij} = \left(\frac{V_i}{RT}\right)(\delta_i - \delta_j)^2 + \gamma \tag{21}$$

is used to estimate the interaction parameter between components i and j. γ is an entropy correction term considered to be a constant near 0.3 when polymer is one of the components in the pair, and set to zero for interaction between the two liquids. Equation (17) is used to estimate the polymer solubility parameter, and eq. (19) for the solubility parameter of the liquid components. Note that eq. (19) is not defined for temperatures above the critical point of the liquid. This poses a problem when considering ethylene polymerization—the reactions are run at temperatures higher than 282.4 K, the critical temperature of ethylene. For propylene polymerization, reaction temperatures are often close to the critical temperature of propylene, 364.9 K.

In both eqs. (20) and (21), it is necessary to estimate the partial molar volumes of the components in the binary liquid mixture. For olefin polymerization, these values are a function of temperature, pressure and composition. Reactions are run at vapour-liquid equilibrium and the binary composition is estimated using the BWR equation of state. Partial molar volumes (V_i) are estimated according to a method proposed by Chueh and Prausnitz,[29] based on a modified Redlich-Kwong correlation. At high pressures in the critical region, V_i is usually a strong function of composition, especially for heavy components for which the value can even change sign due to condensing effects. Partial molar volumes for the heptane-propylene system as a function of propylene mole fraction are shown in Fig. 9 at 30, 60, and 90°C. It can be seen that at propylene mole fractions greater than 0.8, the partial molar volume of heptane starts to drop rapidly. It is expected that this will have a major effect on simulation results in this region.

Finally, in order to solve eq. (20), it is necessary to estimate the volume fraction of polymer in the swollen amorphous phase. The best estimate that could be obtained, as discussed previously, is taken from the fit of experimental data shown in Fig. 8. Note that the data show swelling due to sorption of a single component. Using these data for a binary mixture is equivalent to assuming that the presence of monomer has no effect on the extent of swelling. It is more likely that v_p should be modelled as a function of composition as well as temperature; presently, there are insufficient data to do so.

Using the above parameter estimates, it is possible to solve for the concentration of propylene in the amorphous phase of swollen polypropylene, $[M]^*$, using eq. (20). This concentration can be compared to $[M]_b$, the propylene concentration in the heptane phase. Experimentally it is usually observed that the rate of polymerization is proportional to $[M]_b$. It is necessary to examine whether the same relationship is found when the true concentration of monomer

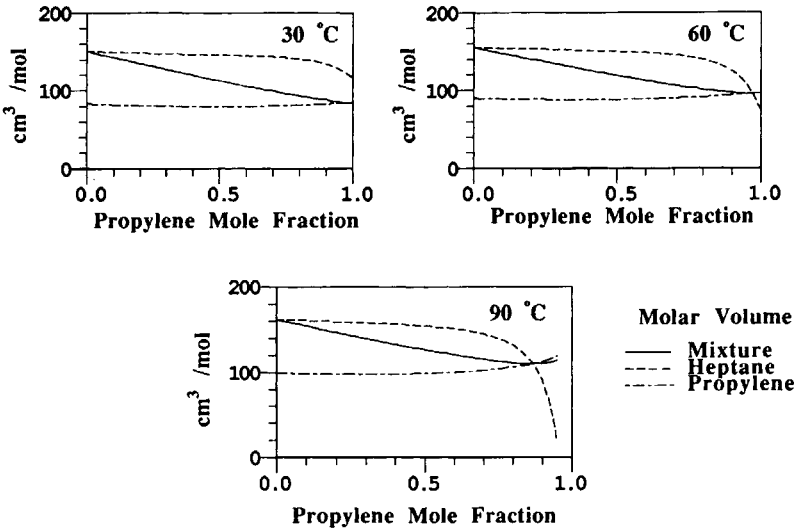

Fig. 9. Partial molar volume (cm^3/mol) of propylene and heptane in a binary mixture.

at the polymer site, $[M]^*$, is used. Simulations were carried out at different temperature levels, varying the propylene mole fraction in the binary phase between zero and one.

Figure 10 shows the results at 60°C, plotting propylene concentrations in both the binary liquid mixture and the swollen amorphous polymer phase as a function of propylene mole fraction in the binary phase. It is immediately evident that the value of $[M]^*$ is much lower than $[M]_b$. This is expected, since the propylene sorbs from a binary to a tertiary phase; there is simply less volume for the propylene to occupy. Also, an examination of the interaction parameters shows that, for all simulations

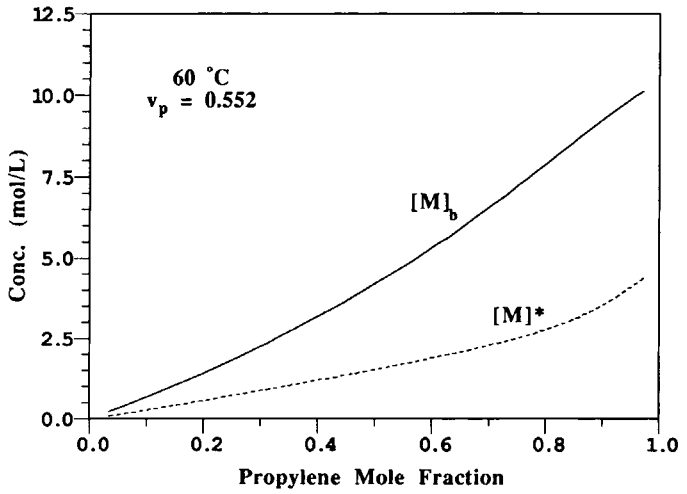

Fig. 10. Propylene concentration versus propylene mole fraction at 60°C: —— Binary propylene-heptane phase ----- Swollen amorphous polymer phase.

$$\chi_{1p} > \chi_{12} > \chi_{2p} \tag{22}$$

where subscript 1 denotes propylene, 2 denotes heptane and "p" denotes the polymer. This order indicates that contact between heptane and polymer is favoured over that between propylene and polymer; heptane is preferentially sorbed.

Figure 11 plots the concentration ratio ($[M]^*/[M]_b$) versus propylene mole fraction at 30, 60, and 90°C. Although all curves cover the mole fraction range from zero to one, the corresponding pressure ranges vary widely with temperature. At 30°C the range is 1–12.5 atm, while at 90°C the range is 1–39.5 atm. If it is assumed that the rate of polymerization is first order in monomer concentration at the active site, then

$$R_{ob} \propto [M]^* \tag{23a}$$

However, as mentioned previously, it is observed experimentally that

$$R_{ob} \propto [M]_b \tag{23b}$$

Thus, the concentration ratio ($[M]^*/[M]_b$) should remain constant at a given temperature as composition changes. At 30 and 60°C the ratio shows slight variation with composition. It can be argued that the deviation predicted would be masked by experimental error, especially since the composition range shown is much wider than is usually examined experimentally. At 90°C, however, the variation is much higher; the ratio drops gradually from 0.3 to 0.06 as propylene fraction increases, then rises rapidly. Very few kinetic experiments have been repeated in slurry at 90°C; thus no data could be found to comment on the validity of this result. The temperature is within 2°C of the critical temperature

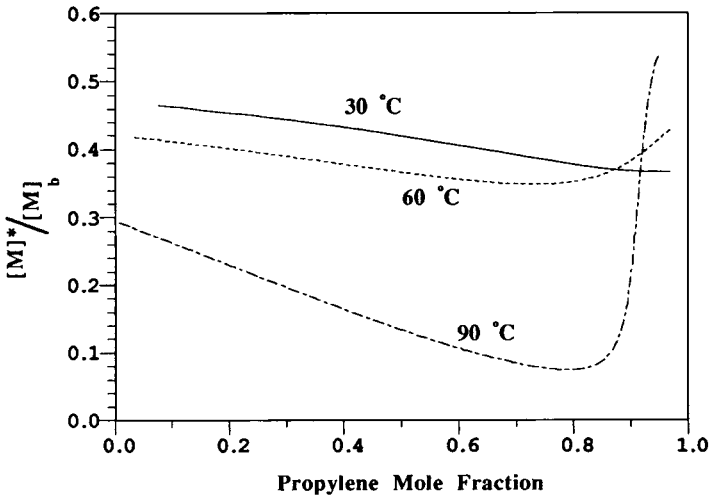

Fig. 11. Propylene sorption in PP from a heptane-propylene liquid mixture: concentration ratio $\left(\frac{[M]^*}{[M]_b}\right)$ versus propylene mole fraction.

of propylene; at this temperature, parameter estimation is more uncertain. For example, Fig. 9 shows that as mole fraction propylene approaches a value of 1, the partial molar volume of the heptane at 90°C falls off towards zero. This behaviour explains the sharp uprise seen in Fig. 11. Because of these uncertainties, K-C theory will not be applied to ethylene slurry polymerizations, in which the reaction temperature is always higher than the critical temperature of the monomer.

As discussed previously, the parameter which is the most difficult to estimate is v_p. Figure 12 shows the effect of varying v_p on the concentration ratio ($[M]^*/[M_b]$) at 30, 60, and 90°C. Simulations shown were done at a pressure of 5 atm. As the value of v_p is increased, the ratio decreases—there is less volume for the monomer to occupy. The rate of decrease is relatively uniform at all temperatures; thus, it can be concluded that although the value of v_p has a quantitative effect on the simulation results, it will not qualitatively affect the trends discussed previously.

GAS VERSUS LIQUID POLYMERIZATION: A COMPARISON

The main motivation for this paper is to present an explanation for the differences in polymerization behaviour seen when the reaction is carried out in various media. It is not easy to predict how a catalyst will perform in a gas phase fluidized bed reactor based on its performance in a bench scale diluent slurry reactor—polymerization rates, temperature behaviour and comonomer incorporation may vary greatly. These observed differences may partially be explained by an examination of monomer sorption behaviour in vapour and liquid reactors. For the two cases of interest, the following points can be summarized:

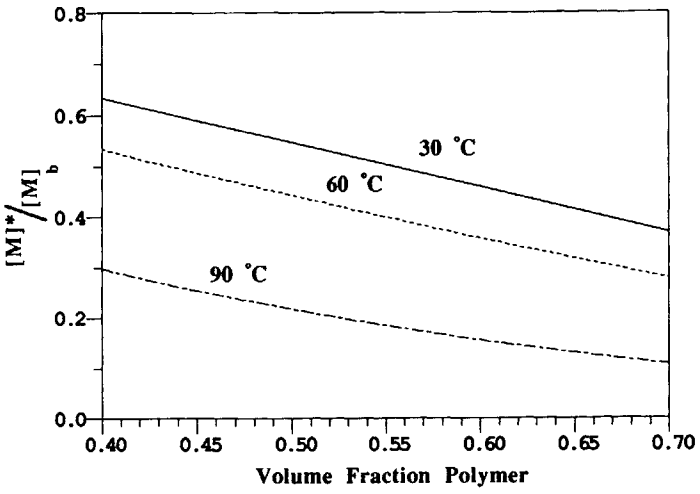

Fig. 12. Propylene sorption in PP from a heptane-propylene liquid mixture: Concentration ratio $\left(\frac{[M]^*}{[M]_b}\right)$ versus v_p at $P = 5$ atm.

Gas Phase

- Monomer condenses during sorption into the polymer phase, changing from a vapour to a liquid. Because of this, the concentration of monomer can actually be higher in the polymer phase than in the gas phase.
- Ethylene and propylene sorption can be modelled by Henry's law, but deviations from this behaviour are predicted for butene and hexene.
- Heavier olefin monomers sorb at least an order of magnitude greater than lighter monomers. The sorption of a heavier monomer can lead to enhanced sorption of a lighter component in a mixture.
- The extent of sorption decreases as temperature increases.

Liquid Phase

- Since the monomer already exists in a condensed state in the reactor diluent, no phase change occurs during the sorption process. Thus, monomer concentrations are lower in the polymer phase than in the liquid phase.
- The sorption of a monomer-diluent slurry can be estimated using K-C theory. Simulations indicate that the diluent is preferentially sorbed into the polymer phase. The swelling of the polymer by the diluent enhances monomer sorption.
- As temperature increases, the ratio of monomer concentration in the polymer phase to reactor monomer concentration decreases. The ratio also becomes more composition dependent as temperature increases.
- Little experimental data is available to verify the K-C theory. Its applicability to mixtures at temperatures close to or above the critical temperature of the monomer is questioned.

Figure 13 examines propylene sorption into polypropylene from gaseous propylene and from a propylene-heptane liquid mixture. Propylene concentration in the polymer phase is plotted as a function of propylene concentration in the

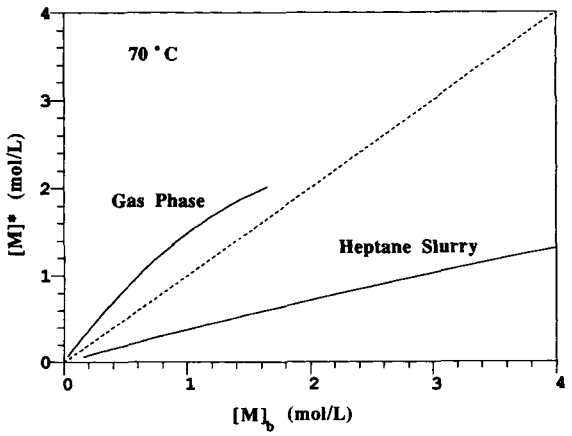

Fig. 13. Estimated concentration of propylene sorbed in polypropylene as a function of propylene reactor concentration: Gas phase and heptane slurry at 70°C.

reactor phase. For sorption from the gas phase it is calculated that $[M]^* > [M]_b$, while for sorption from the liquid mixture the opposite is true. This fact, as well as the other points summarized above, helps to explain some puzzling experimental results seen in the catalyzed olefin polymerization literature.

In the discussion which follows, it is assumed that:

- there are no diffusion limitations in the polymer. While previous results[2] indicate that macroparticle diffusion limitations could be expected for slurry reactors, the rate reduction due to diffusion is small relative to the large differences in intrinsic rates reported for gas and slurry reactors. Thus for the analysis which follows, we neglect both this macroparticle diffusion resistance as well as any microparticle diffusion resistance which might arise.
- polymer at the catalyst surface is 100% amorphous. Evidence suggests that during the reaction successive polymerization and crystallization take place; the polymer chains grow away from the catalyst surface before crystallization can occur.[30,31] This assumption does not indicate that the crystallinity of the polymer is unimportant—crystalline polymer plays an important role in determining the extent of swelling which occurs in the amorphous regions surrounding the catalyst fragments.

Gas versus Diluent Slurry Propylene Polymerization

It is normally observed that polymerization rate is proportional to monomer concentration in the bulk phase, according to

$$R_{ob} = k_p C^* [M]_b \tag{24}$$

Many systems are modelled with an Arrhenius temperature relationship—a plot of $\ln(R_{ob}/[M]_b)$ versus inverse temperature yields a straight line of slope $(-E/R)$. If catalytic activity is equal in gas phase and slurry reactors it would be expected that, for the same catalyst system at the same temperature, the ratio

$$\frac{(R_{ob}/[M])_{\text{gas}}}{(R_{ob}/[M])_{\text{liq}}} = \frac{(k_p C^*)_{\text{gas}}}{(k_p C^*)_{\text{liq}}} = 1 \tag{25}$$

The Arrhenius plots should coincide if the kinetic parameters $(k_p C^*)$ are identical in the two media.

Unfortunately, few studies exist in the literature which characterize the same catalyst system in both gas phase and slurry systems. Three data sets which compare propylene polymerization rates in gas phase and heptane slurry are summarized in Table III. The data of Doi and coworkers,[32,33] reflect the polymerization rate once a stationary rate had been reached, while the third data set[34,35,36] uses four hour average polymerization rates. When Arrhenius plots are constructed using the monomer concentrations in the reactors (in eq. (25), $[M] = [M]_b$) for all cases the normalized gas phase rate is much higher than the normalized slurry rate. The plots are shown as Figures 14a, 15a and 16a. The observed rate differences are too large to be explained by heat or mass

TABLE III
Propylene Polymerization: Gas Phase Versus Diluent Slurry Experimental Conditions

Catalyst system	Medium	Reference	Al/Ti	P (atm)	Range of T (°C)	Reaction rate determination
$TiCl_3$/DEAC	Gas phase	Doi et al.[32]	1.0	1.0	24–53	stationary rate
(Figure 14)	Heptane slurry		1.0	1.0	24–53	(no decay)
$TiCl_3$/TEA	Gas phase	Doi et al.[33]	2.5	1.0	35–46	stationary rate
(Figure 15)	Heptane slurry		2.5	1.0	35–46	(after decay period)
$TiCl_3$/DEAC	Gas phase	Choi and Ray[35]	3.68	7.5	30–90	4 h avg rate
(Figure 16)	Heptane slurry	Yuan et al.[34]	5.0	5.0	30–90	5 h avg rate
	Heptane slurry	Mann[36]	5.0	9.5–17.4	40–80	4 h avg rate

transfer arguments.[3] Note that the plots based on $[M]_b$ indicate large differences in activation energy (cf. Table IV) between gas phase and slurry polymerization.

For the last set of data, there are two series of heptane slurry data, obtained in different reactors.[34,36] The slurry data sets do not coincide, either in level of activity or activation energies. This illustrates some of the problems that can occur when comparing rate data—differences may occur because of impurities or other procedural variations. Mann[36] suggested that another possible explanation is that different batches of the industrial $TiCl_3$ catalyst were used for the two sets of slurry experimentation.

A word should also be said about the activation energies shown in Table IV. The values obtained by Doi et al. are much higher than those obtained for the third comparison set. It has been shown that thermal deactivation of active

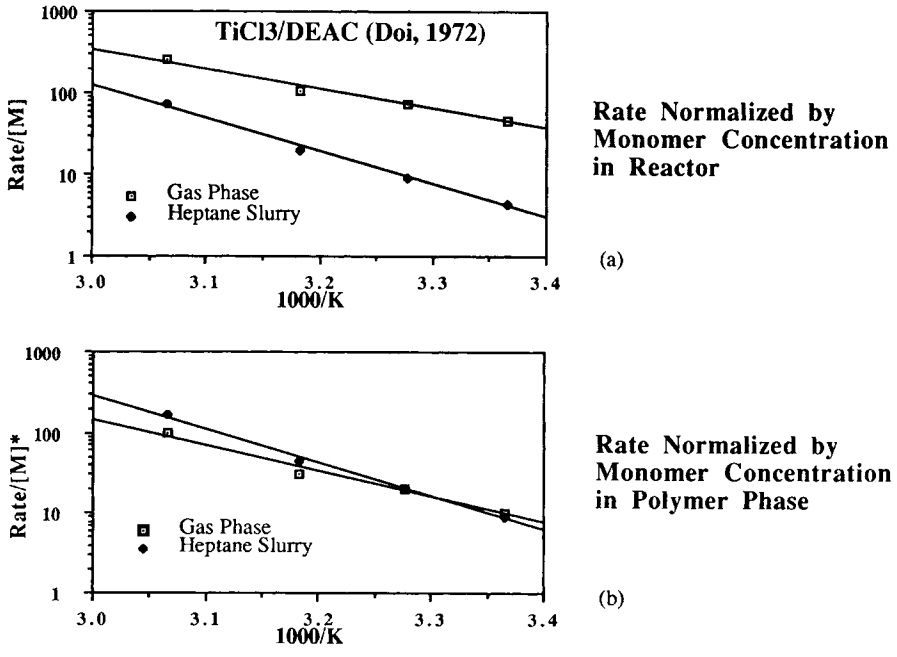

Fig. 14. Arrhenius plot of data of Doi et al.:[32] $TiCl_3$/DEAC (see Table III) (a) Rate normalized by $[M]_b$ (b) Rate normalized by $[M]^*$.

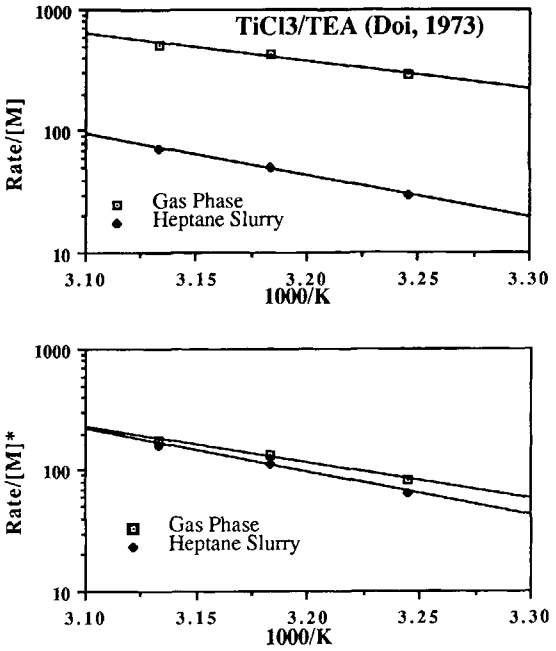

Rate Normalized by Monomer Concentration in Reactor

(a)

Rate Normalized by Monomer Concentration in Polymer Phase

(b)

Fig. 15. Arrhenius plot of data of Doi et al.:[32] $TiCl_3$/TEA (see Table III) (a) Rate normalized by $[M]_b$ (b) Rate normalized by $[M]^*$.

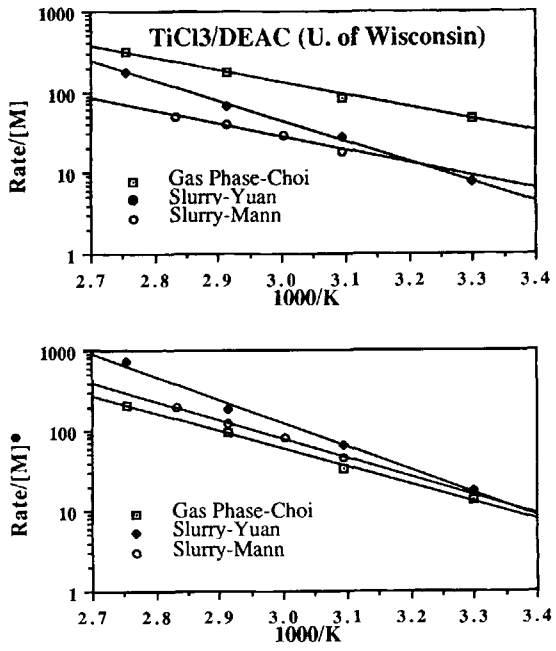

Rate Normalized by Monomer Concentration in Reactor

(a)

Rate Normalized by Monomer Concentration in Polymer Phase

(b)

Fig. 16. Arrhenius plot of 3rd data set: $TiCl_3$/DEAC (see Table III) (a) Rate normalized by $[M]_b$ (b) Rate normalized by $[M]^*$.

TABLE IV
Propylene Polymerization: Gas Phase Versus Diluent Slurry Activation Energies

Catalyst system	Medium	Reference	Activation energy (kcal/mol) Rate normalized by $[M]_b$	Activation energy (kcal/mol) Rate normalized by $[M]^*$
$TiCl_3$/DEAC	Gas phase	Doi et al.[32]	11.2	14.6
(Figure 14)	Heptane slurry		18.4	18.9
$TiCl_3$/TEA	Gas phase	Doi et al.[33]	10.4	13.7
(Figure 15)	Heptane slurry		16.0	16.6
$TiCl_3$/DEAC	Gas phase	Choi and Ray[35]	7.0	10.1
(Figure 16)	Heptane slurry	Yuan et al.[34]	11.4	13.2
	Heptane slurry	Mann[36]	7.4	10.7

sites can cause a decrease in observed activation energies at high temperatures.[3] Cocatalyst concentration may also affect the observed values.[37] As indicated in Table III, the experiments of Doi were run at lower pressures, lower Al/Ti ratios and over lower (and narrower) temperature ranges. Also, Doi's data reflect an instantaneous rate of reaction at a specified time, instead of an average rate of polymerization. These experimental differences provide some possible explanations for the different activation energies.

It is postulated that the observed rate differences seen in Figs. 14–16 are not due to different intrinsic activities, but can be explained through sorption theory. In eq. (25), instead of normalizing the observed rates by the monomer concentration in the reactor, the actual monomer concentration at the catalyst surface should be used. Under the assumptions mentioned previously, this is simply the sorbed concentration of propylene in amorphous polypropylene, $[M]^*$. Results of this renormalization are shown in Figs. 14b, 15b, and 16b. For all cases, the gas phase and liquid slurry curves are much closer together. Figure 16b, with the two sets of slurry data, once again has the most scatter. Accounting for monomer sorption also leads to a narrowing of the gap between activation energies observed in the gas and liquid reactors, as summarized in Table IV. In general, considering the uncertainty in estimating sorbed concentrations, the agreement is excellent. It appears as if sorption effects are the major cause of the observed differences in intrinsic rate between gas phase and slurry reactors for the same catalyst system. Understanding these effects will make scale-up between liquid and gas phase reactors much easier to predict.

Gas versus Diluent Slurry Ethylene Polymerization

For ethylene slurry polymerization, it is difficult to estimate the necessary parameters for the Krigbaum-Carpenter theory, since operating temperatures are above the critical temperature of the monomer. Because of this, a comparison between gas phase and slurry ethylene polymerizations is difficult to make. For liquid polymerization, it appears as if polyethylene is swollen to a lesser extent by liquid hexane than polypropylene is by heptane (Fig. 8). This suggests that ethylene concentrations in amorphous polymer during slurry polymerizations will be low. For gas phase polymerization, eqs. (4) and (14) can be used to

estimate monomer concentrations in the amorphous polymer surrounding the catalyst sites.

Copolymerization

Recently, much attention has been drawn to the area of copolymerization. For many catalyst systems, adding a small amount of α-olefin comonomer leads to a significant increase of ethylene consumption. Figure 17 is a typical example.[38] When hexene is added to the ethylene-hexane system, the maximum activity increases by a factor more than three. The profile of the rate curve changes dramatically also.

Rate enhancement is seen for copolymerization reactions in gas phase reactors,[39] for diluent slurry reactors,[38,46,47] and even for some solution polymerization systems.[42] The reason for this enhancement is not clear. Tait et al.[43] show that the presence of comonomer leads to an increase in the number of active polymerization sites for a number of catalysts in slurry phase; both kinetic (activation of new sites) and physical (better catalyst breakup, less site blockage due to lower crystallinity) explanations were offered. Ray[44] suggests that polymer of lower crystallinity leads to an increased rate of monomer diffusion, and thus enhanced reaction rate. Munoz-Escalona et al.[45] have also adopted this view. However, since rate enhancement is also observed in solution polymerization, it is expected that the increased rate is largely a kinetic phenomenon.

In spite of these other factors, it is useful to examine the part that monomer sorption plays in the observed rate enhancement. Most of the studies mentioned above were carried out in the slurry phase, such as the data of Calabro and Lo[38] (Fig. 17). Sorption arguments cannot be used to explain the threefold

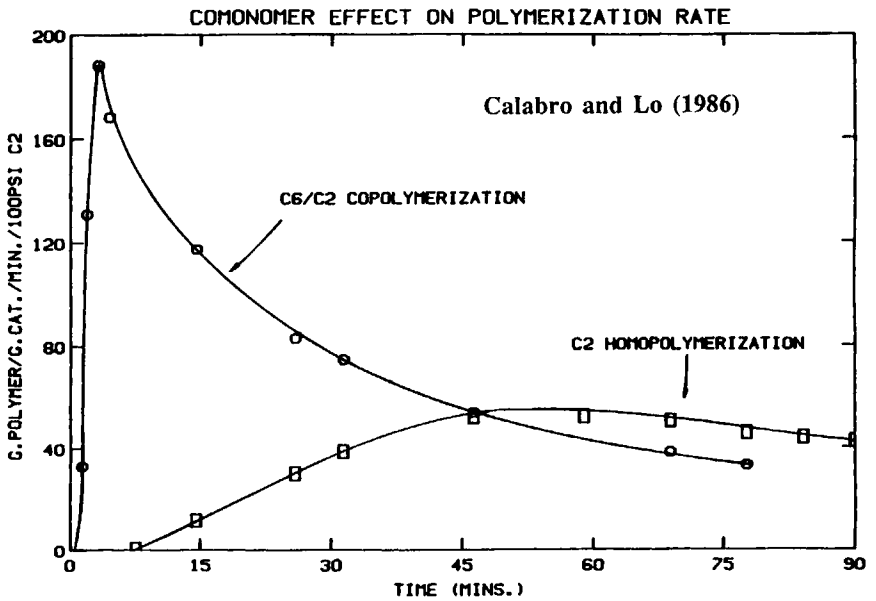

Fig. 17. Rate profiles for ethylene homopolymerization and copolymerization with hexene, in hexane slurry: 80°C, 120 psig, Mg/Ti/SiO_2 catalyst.[38]

increase in reaction rate for this system. Since the polymer is already swollen to a great extent by hexane, it is not likely that the addition of a small amount of hexene will lead to an enhanced sorption of ethylene. It should be noted, however, that as comonomer content in the polymer increases, the polymer crystallinity decreases. With lower crystallinity, fewer crystallite "crosslinks" are present to restrict the swelling of the amorphous polymer. This will lead to a slight increase in the monomer concentration in the swollen polymer phase. Lower crystallinity also leads to increased diffusion rates, which will result in higher polymerization rates if the reaction is diffusion controlled.

For gas phase polymerizations the situation is different. Unlike slurry polymerization, there is no diluent present to swell the polymer. The addition of a comonomer (e.g. hexene or butene) which has a high solubility in polymer will lead to enhanced solubility of the lighter ethylene component, as shown by Li and Long[12] and Robeson and Smith.[19] As the comonomer/monomer ratio increases, increased swelling and ethylene sorption should be seen, leading to a higher polymerization rate. Note that this increased swelling should occur independent of the polymer crystallinity. According to this argument, therefore, a rate increase should also be seen if an inert (butane or hexane) is used to swell the polymer instead of the comonomer. Sorption theory also suggests that an increased rate enhancement will be observed as progressively heavier comonomers are used; for example, hexene (or hexane) will swell the polymer to a greater extent than butene (or butane). Experimental examination of these hypotheses should not be difficult; however, no systematic study has been found which looks at these trends.

Understanding the sorption process is important when considering another aspect of copolymerization—comonomer incorporation. The amount of comonomer incorporated in the final polymer product can be related to the relative monomer concentrations in the reactor according to

$$\left(\frac{M_\alpha}{M_{\text{eth}}}\right)_{\text{poly}} = \frac{1}{r_1}\left(\frac{[M_\alpha]_b}{[M_{\text{eth}}]_b}\right) \tag{26}$$

where r_1 is the reactivity ratio of copolymerization constants k_{11}/k_{12} (1 = ethylene, 2 = α-olefin). This equation is a simplification of the Mayo copolymer composition relation, assuming the following: (a) the ratio of monomer concentrations is constant with time; (b) the reactivity ratio $r_2 = k_{22}/k_{21}$ is much smaller than $[M_{\text{eth}}]/[M_\alpha]$; (c) copolymer content incorporated in the polymer is low. These assumptions are valid for normal conditions employed in the production of linear-low density polyethylene. Bukatov et al.[39] have used eq. (26) to examine the reactivity ratios of ethylene with propylene and butene in both gas phase (80°C) and hexane slurry (70°C) reactors using a Mg-supported Ti catalyst (cf. Table V). It can be seen that the "observed" reactivity ratio r_1, based on bulk conditions, is much lower in the gas phase system. This implies that, for the same catalyst system, comonomer incorporation occurs to a higher level in the gas phase than in slurry. As suggested by Bukatov et al.,[39] this difference is seen because monomer sorption has not been taken into account. The actual reactivity ratio (r_1^*) should be calculated using the monomer concentrations in the polymer phase, according to

TABLE V
Reactivity Ratios for Ethylene–α-Olefin Copolymerization with $TiCl_4/MgCl_2$ + AlR_3 (Bukatov et al.[39])

	Reactivity ratios	
	Ethylene-propylene	Ethylene-butene
Hexane slurry (70°C): r_1-based on monomer conc. in reactor	13	29
Gas phase (80°C): r_1-based on monomer conc. in reactor	3.2	2.4
Hexane slurry (70°C): r_1^*-based on monomer conc. in polymer	13	29
Gas phase (80°C): r_1^*-based on monomer conc. in polymer (Bukatov[39])	12.8	24.0
Gas phase (80°C): r_1^*-based on monomer conc. in polymer (this work)	9.3	16.4

$$\left(\frac{M_\alpha}{M_{\text{eth}}}\right)_{\text{poly}} = \frac{1}{r_1^*}\left(\frac{[M_\alpha]^*}{[M_{\text{eth}}]^*}\right) \tag{27}$$

For ethylene slurry polymerization, as mentioned previously, it is difficult to estimate the concentration of monomers in the polymer phase. Thus it is necessary to assume that comonomer ratio does not change during sorption ($r_1^* = r_1$). This assumption is reasonable as a first approximation, since most of the polymer swelling is caused by the diluent. For gas phase reactors, however, it is known that the heavier component is preferentially sorbed. Based on the experimental work of Michaels and Bixler,[9] Bukatov et al.[39] estimated the change in monomer concentration ratios as

$$\frac{[M_{\text{prop}}]^*/[M_{\text{eth}}]^*}{[M_{\text{prop}}]_b/[M_{\text{eth}}]_b} = 4, \qquad \frac{[M_{\text{but}}]^*/[M_{\text{eth}}]^*}{[M_{\text{but}}]_b/[M_{\text{eth}}]_b} = 10 \tag{28}$$

This correction brings the gas phase reactivity ratios much closer to the level observed for the slurry reactions (Table V).

The modelling discussed in this paper provides a means of estimating the ratio of concentrations in the amorphous phase for any comonomer pair in gas phase. According to eqs. (4) and (14),

$$\frac{[M_\alpha]^*}{[M_{\text{eth}}]^*} = R\left(\frac{P_\alpha}{P_{\text{eth}}}\right) \tag{29}$$

where

$$\log R = \frac{-1.08}{T^2}\left((T_{c\alpha})^2 - (T_{c\text{eth}})^2\right) \tag{30}$$

It should be remembered that this is strictly valid only for systems which obey Henry's Law. Since, as mentioned previously, sorption of the heavier α-olefin monomer leads to increased sorption of the ethylene, eq. (30) only provides a rough estimate of the relative sorption of the two monomers in the polymer phase. Values of R have been tabulated as a function of temperature for various ethylene—α-olefin pairs in Table VI. Since

$$\frac{[M_\alpha]_b}{[M_{\text{eth}}]_b} \approx \frac{P_\alpha}{P_{\text{eth}}} \tag{31}$$

the relation between observed and true reactivity ratio is

$$r_1^* = Rr_1 \tag{32}$$

Equation (32) has been applied to the gas phase data of Bukatov et al.[39] at 80°C (Table V). Although different from the predicted values of Bukatov, agreement is still good, especially considering the temperature difference between the gas and slurry experiments.

As illustrated in the above example, with gas phase polymerization it is possible to achieve high comonomer incorporation due to the enhanced sorption of the heavier α-olefin. Table VI indicates that octene vapour is preferentially sorbed (relative to ethylene) into the polymer phase by a factor greater than two orders of magnitude. A patent to Phillips[50] further illustrates this point. For a Cr-Ti on silica catalyst, the relationship between comonomer content in the polymer and in the reactor was expressed as follows

$$\left(\frac{M_\alpha}{M_\alpha + M_{\text{eth}}}\right)_{\text{poly}} = k\left(\frac{[M_\alpha]_b}{[M_\alpha]_b + [M_{\text{eth}}]_b}\right) \tag{33}$$

Since comonomer mole fractions in both the polymer product and the reactor are small, this can be simplified to eq. (26), with $r_1 = 1/k$. Values of the reactivity ratio (r_1) calculated by eq. (33) for various ethylene—α-olefin systems are shown in Table VII. The value for butene compares favourably to the r_1 value of 1.3 obtained by Bukatov et al.[39] for a similar Cr on silica catalyst. Two

TABLE VI
Values of R, the Ratio of True to Apparent Reactivity Ratios for Ethylene—α-Olefin Gas Phase Polymerization Systems

	Comonomer				
T (°C)	Propylene	Butene	Hexene	Octene	4-Methyl-1-pentene
50	3.57	9.91	63.4	312.9	48.9
60	3.31	8.65	49.5	222.8	38.8
70	3.09	8.65	39.7	163.3	31.5
80	2.90	6.82	32.3	122.9	25.9
90	2.74	6.15	26.7	94.6	21.7

TABLE VII
Reactivity Ratios for Gas Phase Polymerization over a Cr/Ti Silica-Supported Catalyst (U.S. Patent[50])

Comonomer	r_1: based on $[M_\alpha]/[M_{eth}]$ in reactor	r_1^*: based on $[M_\alpha]^*/[M_{eth}]^*$ in polymer phase (80°C)
Butene	0.83–1.7	5.7–11.4
Hexene	0.40–0.71	12.9–23.1
Octene	0.14–0.25	17.6–30.7
4-Methyl-1-pentene	0.71–1.0	18.5–25.9

interesting facts can be noted from the data of Table 7. It can be seen that the values of r_1 decrease as heavier comonomers are used; octene has a better observed incorporation rate than butene. Also, most of the r_1 values are less than unity, indicating that the comonomer fraction in the final polymer product is higher than the comonomer fraction in the reactor. Both of these results contradict the known literature data on the relative kinetic reactivity of ethylene and heavier α-olefins. In order to understand this data and to calculate the true reactivity ratios, monomer sorption must be considered. Equation (32) has been used to calculate the true reactivity ratios (r_1^*) at 80°C and the values are also shown in Table 7. It is only after correcting for sorption effects that the experimental results make sense; the r_1^* values in Table 7 exhibit the expected kinetic trends, with $r_1^* > 1$ and r_1^* increasing as heavier comonomers are used.

It can be seen that sorption effects play an important role during gas phase copolymerization. Without understanding this, scale-up from hexane slurry to gas phase copolymerization will result in very different comonomer levels in the polymer product than expected. Figure 18 shows the relationship between

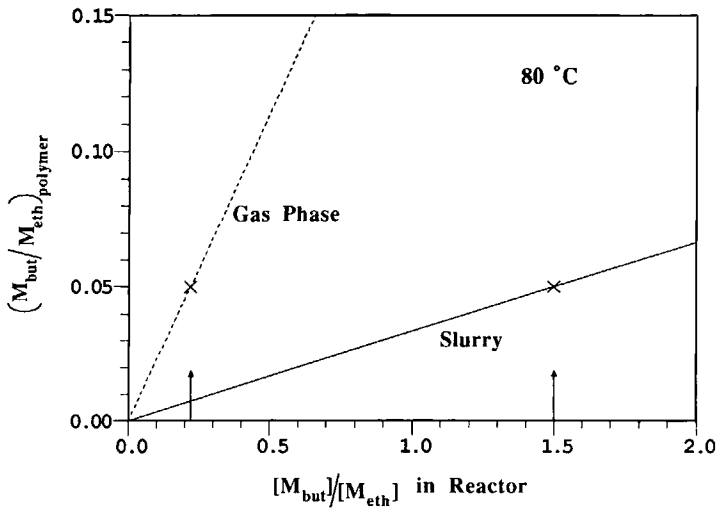

Fig. 18. An example of enhanced comonomer incorporation due to monomer sorption effects: Butene-Ethylene copolymerization (80°C).

comonomer level incorporated into the polymer and comonomer ratio in the reactor for an ethylene-butene copolymerization at 80°C, assuming a true reactivity ratio (r_1^*) of 30. In a slurry reactor, to produce a polymer with a comonomer mole fraction of 0.05 the concentration ratio of monomers in the liquid reactor ($[M_{but}]/[M_{eth}]$) needs to be 1.5 ($r_1 = r_1^*$). Without considering monomer sorption effects, it would be expected that the same concentration ratio (P_{but}/P_{eth}) is necessary in a gas phase reactor to maintain the same level of comonomer incorporation. This is incorrect, however; it is necessary to correct for gas phase sorption effects. Using eq. (32) and Table VI, at 80°C the apparent gas phase reactivity ratio, r_1, is calculated to be 4.4 (30/6.82). This apparent reactivity ratio has been used in the construction of the second curve shown in Fig. 18. It is only necessary to have a gas phase ratio (P_{but}/P_{eth}) of 0.22 in order to get the desired 5% butene incorporation in the polymer. A plot similar to Fig. 18 can be constructed for any copolymerization system, and should prove to be very useful in predicting the level of comonomer incorporation in a gas phase reactor based on results obtained in a diluent slurry reactor.

CONCLUSIONS

Understanding the process of monomer sorption is essential when trying to predict catalyst behaviour in different reactor media. Monomer concentrations in the polymer phase at the catalyst surface are much different than bulk reactor concentrations. Using available theory to calculate these local concentrations leads to a more unified picture of catalyst behaviour, both in terms of reaction rates and comonomer incorporation. It is likely that the predictive capabilities of our monomer sorption expressions can be improved greatly through the use of more sophisticated thermodynamic theories and more thermodynamic and kinetic data. Further research in this direction is underway.

We are grateful to the National Science Foundation and to the industrial sponsors of the University of Wisconsin Polymerization Reaction Engineering Laboratory for research support. One of the authors (RAH) would also like to thank the Natural Sciences and Engineering Research Council of Canada for financial support.

APPENDIX: NOMENCLATURE

a_i	vapour activity of component i
C^*	catalyst active site concentration
E	activation energy (kcal/mol)
K	Krigbaum-Carpenter partition coefficient for binary liquid sorption
k^*	vapour solubility coefficient (mol/L-amorphous polymer/atm)
k_p	propagation rate constant
$[M]^*$	monomer concentration in amorphous polymer (mol/L)
$[M]_b$	monomer concentration in reactor (mol/L)
P_c	critical pressure (atm)
P_{dev}	pressure at which 5% deviation from Henry's Law is seen (atm)
P_i	partial pressure of component i (atm)
P_i^0	saturation pressure of component i (atm)
R	relative enhancement coefficient for gas phase copolymerization ($\approx r_1^*/r_1$)
r_1	observed reactivity ratio, based on monomer concentrations in reactor

r_1^* actual reactivity ratio, based on monomer concentrations in amorphous polymer
R_{ob} polymerization rate (g polymer/g cat/hr)
T_c critical temperature (K)
T_r reduced temperature (T/T_c)
V_i partial molar volume of component i (cm^3/mol)
v_i volume fraction of component i in swollen amorphous polymer
v_p polymer volume fraction in swollen amorphous polymer
α_v polymer amorphous volume fraction
χ_{ij} Flory interaction parameter between components i and j
δ_i solubility parameter of component i $(cal/cm^3)^{1/2}$
ϕ_i volume fraction of component i in binary liquid phase
ρ polymer density (g/cm^3)
ρ_a density of 100% amorphous polymer (g/cm^3)
ρ_c density of 100% crystalline polymer (g/cm^3)

References

1. Floyd, S., K.-Y. Choi, T. W. Taylor, and W. H. Ray, *J. Appl. Polym. Sci.*, **32,** 2231 (1986a).
2. Floyd, S., K.-Y. Choi, T. W. Taylor, and W. H. Ray, *J. Appl. Polym. Sci.*, **32,** 2935 (1986b).
3. Floyd, S., T. Heiskanen, T. W. Taylor, G. E. Mann, and W. H. Ray, *J. Appl. Polym. Sci.*, **33,** 1021 (1987).
4. Hock, C. W., *J. Polym. Sci. A-1,* **4,** 3055 (1966).
5. Wilchinsky, Z. W., R. W. Looney, and E. G. M. Tornqvist, *J. Catal.* **28,** 351 (1973).
6. Kakugo, M., H. Sadatoshi, M. Yokoyama, and K. Kojima, *Transition Metals and Organometallics as Catalysts for Olefin Polymerization,* W. Kaminsky and H. Sinn, Eds., Springer-Verlag, Berlin, 1988, p. 433.
7. Stannett, V. and H. Yasuda, *Crystalline Olefin Polymers Part II,* R. M. V. Raff and K. W. Daak, Eds., Interscience Publishers, New York, 1964, p. 131.
8. Rogers, C. E., V. Stannett, and M. Szwarc, *J. Polym. Sci.*, **45,** 61 (1960).
9. Michaels, A. S. and H. J. Bixler, *J. Polym. Sci.*, **50,** 393 (1961).
10. Frensdorff, H. K., *J. Polym. Sci. A-2,* **2,** 333 (1964).
11. Ito, K. and J. E. Guillet, *Macromolecules,* **12,** 1163 (1979).
12. Li, N. N. and R. B. Long, *AIChE J.*, **15,** 73 (1969).
13. Kulkarni, S. S. and S. A. Stern, *J. Polym. Sci., Polym. Phys. Ed.*, **21,** 441 (1983).
14. Liu, C.-P. A. and P. Neogi, *J. Membrane Sci.*, **35,** 207 (1988).
15. Teplyakov, V. V. and S. G. Durgar'yan, *Polym. Sci. USSR,* **28,** 629 (1986).
16. Abraham, M. H., et al., *Polymer,* **28,** 1363 (1987).
17. Stern, S. A., J. T. Mullhaupt, and P. J. Gareis, *AIChE J.*, **15,** 64 (1969).
18. Meyer, J. A., C. Rogers, V. Stannett, and M. Szwarc, *Tappi,* **40,** 142 (1957).
19. Robeson, L. M. and T. G. Smith, *J. Appl. Polym. Sci.*, **12,** 2083 (1968).
20. Rogers, C. E., V. Stannett, and M. Szwarc, *Tappi,* **41,** 715 (1961).
21. Fels, M. and R. Y. M. Huang, *J. Appl. Polym. Sci.*, **14,** 537 (1970).
22. Michaels, A. S., W. Vieth, A. S. Hoffman, and H. A. Alcalay, *J. Appl. Polym. Sci.*, **13,** 577 (1969).
23. Michaels, A. S., W. Vieth, and H. H. Alcalay, *J. Appl. Polym. Sci.*, **12,** 1621 (1968).
24. Barton, A. F. M., *CRC Handbook of Solubility Parameters and Other Cohesion Parameters,* CRC Press, Inc., Boca Raton, FL, (1983).
25. Fels, M. and R. Y. M. Huang, *J. Macromol. Sci.-Phys.*, **B5,** 89 (1971).
26. Krigbaum, W. G. and D. K. Carpenter, *J. Polym. Sci.*, **14,** 241 (1954).
27. Gardon, J. L., *J. Polymer Sci. A-1,* **6,** 2859 (1968).
28. Guillot, J., *J. Makromol. Chem. Rapid Commun.*, **1,** 697 (1980).
29. Chueh, P. L. and J. M. Prausnitz, *AIChE J.*, **13,** 1099, (1967).
30. Marchessault, R. H., B. Fisa, and H. D. Chanzy, CRC *Crit. Rev. Macromol. Sci.*, **1,** 315 (1972).
31. Munoz-Escalona, A. and A. Parada, *Polymer,* **20,** 859 (1979).
32. Doi, Y., Y. Yoshimoto, and T. Keii, *Nippon Kagaku Kaishi,* **496** (1972).
33. Doi, Y., H. Kobayashi, and T. Keii, *Nippon Kagaku Kaishi,* **1089** (1973).
34. Yuan, H. G., T. W. Taylor, K.-Y. Choi, and W. H. Ray, *J. Appl. Polym. Sci.*, **27,** 1691 (1982).

35. Choi, K.-Y. and W. H. Ray, *J. Appl. Polym. Sci.*, **30,** 1065 (1985).
36. Mann, G. E., M.S. Thesis, U. of Wisconsin-Madison (1985).
37. Yoon, J.-S. and W. H. Ray, *I&EC Research,* **26,** 45 (1987).
38. Calabro, D. C. and F. Y. Lo, paper presented at *Transition Metal Catalyzed Polymerization Symposium,* Akron, 1986.
39. Bukatov, G. D., L. G. Yechevskaya, and V. A. Zakharov, *Transition Metals and Organometallics as Catalysts for Olefin Polymerization,* W. Kaminsky and H. Sinn, Eds., Springer-Verlag, Berlin, 1988, p. 101.
40. McCall, D. W. and W. P. Slichter, *J. Am. Chem. Soc.,* **80,** 1861 (1958).
41. Long, R. B., *I&EC Fundamentals,* **4,** 445 (1965).
42. Schmidt, G. F. and W. M. Coleman, paper presented at *Transition Metal Catalyzed Polymerization Symposium,* Akron, 1986.
43. Tait, P. J. T., G. W. Downs, and A. A. Akinbami, paper presented at *Transition Metal Catalyzed Polymerization Symposium,* Akron, 1986.
44. Ray, W. H., paper presented at *Transition Metal Catalyzed Polymerization Symposium,* Akron, 1986.
45. Munoz-Escalona, A., H. Garcia, and A. Albornoz, *J. Appl. Polym. Sci.,* **34,** 977 (1987).
46. Finogenova, L. T., V. A. Zakharov, A. A. Buniyat-Zade, G. D. Bukatov, and T. K. Plaksunov, *Polym. Sci. USSR* **22,** 448 (1980).
47. Lin, S., H. Wang, Q. Zhang, Z. Lu, and Y. Lu, *Catalytic Polymerization of Olefins,* T. Keii and K. Soga, Eds., Kodansha Ltd., Tokyo, 1986, p. 91.
48. Takeuchi, Y. and H. Okamura, *J. Chem. Eng. Japan,* **9,** 136 (1976).
49. Bradford, M. L. and G. Thodos, *Can. J. Chem. Eng.,* **44,** 345 (1966).
50. U.S. Patent 4,522,987 (1985), to Phillips Petroleum Co.
51. MacDonald, R. W. and R. Y. M. Huang, *J. Appl. Polym. Sci.,* **26,** 2239 (1981).
52. Castro, E. F., E. E. Gonzo, and J. C. Gottifredi, *J. Membrane Sci.,* **31,** 235 (1987).
53. Eby, R. K., *J. Appl. Phys.,* **35,** 2720 (1964).

Received March 27, 1989
Accepted August 9, 1989